**Environmental photodegradation of emerging contaminants: A re-examination of the importance of triplet-sensitised processes, based on the use of 4-carboxybenzophenone as proxy for the chromophoric dissolved organic matter**

# Environmental photodegradation of emerging contaminants: A re-examination of the importance of triplet-sensitised processes, based on the use of 4-carboxybenzophenone as proxy for the chromophoric dissolved organic matter

**Luca Carena,[a] Cezara G. Puscasu,[a] Silvia Comis,[a] Mohamed Sarakha,[b] Davide Vione [a,*]**

[a] *Dipartimento di Chimica, Università di Torino, Via Pietro Giuria 5, 10125 Torino, Italy.*

[b] *Institut de Chimie de Clermont-Ferrand, Clermont Université, Université Blaise Pascal, F-63177 Aubière, France.*

* Corresponding author. E-mail: *davide.vione@unito.it*

## *Abstract*

The photoreactions sensitised by the excited triplet states of chromophoric dissolved organic matter ($^3$CDOM*) are very important in the photochemical attenuation of emerging contaminants in natural waters. Until quite recently, anthraquinone-2-sulphonate (AQ2S) was the only available CDOM proxy molecule to estimate the contaminant reaction kinetics with $^3$CDOM*, under steady-state irradiation conditions. Unfortunately, the AQ2S triplet state ($^3$AQ2S*) is considerably more reactive than average $^3$CDOM*. We have recently developed an alternative protocol based on 4-carboxybenzophenone (CBBP), the triplet state of which ($^3$CBBP*) is less reactive compared to $^3$AQ2S*. Here we show that in the case of ibuprofen (IBP), paracetamol (APAP) and clofibric acid

(CLO), the reaction rate constants with $^3$CBBP* are more reasonable as $^3$CDOM* reactivity estimates than those obtained by using AQ2S. In contrast, similar rate constants are measured for the reaction of atrazine (ATZ) with either $^3$AQ2S* or $^3$CBBP*. Moreover, the reactivity of ATZ with both $^3$AQ2S* and $^3$CBBP* is very similar to that with $^3$CDOM*, available through a literature estimate. The possibility to validate the ATZ-$^3$CBBP* reactivity estimate against the $^3$CDOM* data, and to accurately predict the reported IBP and CLO field lifetime, support the suitability of CBBP as CDOM proxy. The replacement of AQ2S with CBBP as proxy molecule does not reverse the qualitative prediction, according to which $^3$CDOM* would be the main process involved in the photodegradation of the studied contaminants in waters with high dissolved organic carbon (DOC). However, the CBBP-based data prompt for an important reconsideration of the estimated lifetimes at high DOC.

***Keywords:*** Photochemistry; Photochemical modelling; CDOM; DOM antioxidant effect; Water pollutants.

## Introduction

Photochemical reactions are important transformation pathways involved in the degradation of pollutants and of naturally occurring molecules such as amino acids, peptides and proteins. Photochemistry is usually in competition with biodegradation and with abiotic processes including hydrolysis, and it can be the main degradation route for biologically recalcitrant compounds such as several of the so-called contaminants of emerging concern (CECs) (Remucal, 2014; Challis et al., 2014; Yan and Song, 2014; Yassine et al.,2018; Kovacic et al., 2019).

The photoreaction pathways include the direct photolysis, where the substrate absorbs sunlight and gets transformed as a consequence (Iesce et al., 2019), and indirect photochemistry. In the latter,

sunlight is absorbed by naturally occurring molecules called photosensitisers, which produce reactive transient species in aqueous solution when irradiated. The photogenerated transients are then involved in pollutant phototransformation (Burns et al., 2012; Rosario-Ortiz and Canonica, 2016). The main photosensitisers occurring in surface waters are nitrate, nitrite and the chromophoric dissolved organic matter (CDOM, i.e., the light-absorbing fraction of the organic matter dissolved in natural waters), which is in part made up of humic substances. The main transients are hydroxyl ($^{\bullet}OH$) and carbonate ($CO_3^{\bullet-}$) radicals, singlet oxygen ($^1O_2$), and CDOM triplet states ($^3$CDOM*) (Vione et al., 2014; Bahnmueller et al., 2014).

While all the transients are involved to some extent in the phototransformation of contaminants, some photochemical pathways may sometimes induce the formation of peculiar intermediates of considerable health and/or environmental concern (Cermola et al., 2005). For instance, the antimicrobial triclosan yields a dioxin upon both direct photolysis and $^3$CDOM* reaction (Kliegman et al., 2013; Bianco et al., 2014), the antibiotic cefazolin produces toxic species by direct photolysis (Wang and Lin, 2012), and phenylurea herbicides yield toxic N-formyl species upon $^{\bullet}OH$ reaction (Galichet et al., 2002; Bonnemoy et al., 2004). Another issue is that the type and kinetics of photoreactions depend on water chemistry, and particularly on the dissolved organic carbon (DOC) levels. Actually, $^{\bullet}OH$ and $CO_3^{\bullet-}$ are consumed by organic compounds, and the associated processes prevail at low DOC. In contrast, $^3$CDOM* and $^1O_2$ are produced by irradiated CDOM, and the relevant photoreactions are enhanced when the DOC is high (Vione et al., 2014). The direct photolysis is inhibited in the presence of radiation-absorbing organic compounds, but the extent of the direct photolysis inhibition with increasing DOC is usually lower compared to the inhibition of the $^{\bullet}OH$ and $CO_3^{\bullet-}$ processes. Therefore, the direct photolysis is often most significant at intermediate DOC values (Calza et al., 2017).

High DOC levels that enhance $^3$CDOM* reactions can be found in eutrophic water environments. Moreover, such conditions are quite common at elevated Nordic latitudes, which are also the most lake-rich regions of our planet (Verpoorter et al., 2014). The water of many boreal lakes is also

undergoing the so-called browning phenomenon, i.e., a gradual increase in the levels of both DOC and CDOM because of the combined effects of climate change, recovery from acid rain and land-use changes (Williamson et al., 2015; Weyhenmeyer et al., 2016). Water browning is expected to further increase in the future, thus the conditions of many world's lakes will become even more favourable to $^3$CDOM* reactions than they are at the moment (Koehler et al., 2018; Vione and Koehler, 2018). Unfortunately, the nature of the $^3$CDOM* states is not yet completely understood, and the study of the reactivity between $^3$CDOM* and CECs faces several difficulties (McNeill and Canonica, 2016).

The main problem is that CDOM is a mixture of (at least) thousands of compounds, and $^3$CDOM* is thus a lumped notation that encompasses triplet states with very variable nature and reactivity. Recent studies have proposed innovative methods to measure the quenching rate constants of whole $^3$CDOM* by CECs, exploiting the ability of CECs to inhibit some peculiar reactions in which most $^3$CDOM* states are involved (Schmitt et al., 2017; Erickson et al., 2018). These new methods are based on the laser flash photolysis technique but, unfortunately, they do not distinguish between physical and chemical quenching. Indeed, the quenching rate constants thus obtained are upper limits for the reaction rate constants that can be measured by means of steady irradiation experiments (Carena et al., 2017). Nevertheless, some reaction rate constants of $^3$CDOM* with pollutants are actually available, and they have been obtained in steady-irradiation experiments of actual CDOM with addition of scavengers of additional transient species (e.g., $^1O_2$ and $^\bullet$OH). Such species are produced by irradiated CDOM alongside with $^3$CDOM* (Zeng and Arnold, 2013). With this approach, however, there might be issues connected with the selectivity of the scavengers, which could also consume a non-negligible fraction of $^3$CDOM*.

An alternative approach is based on the use of proxy molecules, which should: *(i)* have comparable structure as the $^3$CDOM* precursors within CDOM; *(ii)* produce triplet states under irradiation with comparable reactivity as $^3$CDOM*, and *(iii)* allow for the definition of easily workable protocols to determine the second-order reaction rate constants of the triplet states with CECs. A first example

of proxy has been anthraquinone-2-sulphonate (AQ2S), which does not yield interfering transient species such as $^{\bullet}OH$ or $^{1}O_2$ under irradiation (Bedini et al., 2012). For AQ2S, a straightforward protocol exists for the measurement of the second-order reaction rate constants with its triplet state, $^{3}$AQ2S* (Marchetti et al., 2013). Unfortunately, there is evidence that $^{3}$AQ2S* is more reactive than average $^{3}$CDOM*. Therefore, the assessment of the reactivity between CECs and $^{3}$AQ2S* may lead to overestimations of the role of triplet-sensitised processes in environmental photochemistry (Avetta et al., 2016). For some CECs, anyway, an important role of $^{3}$CDOM* in photodegradation could be excluded even on the basis of $^{3}$AQ2S* reactivity data (Calza et al., 2017).

Interestingly, evidence is available that 4-carboxybenzophenone (CBBP) may be a more suitable proxy molecule than AQ2S (Avetta et al., 2016). We have recently developed an experimental protocol for the measurement of the second-order reaction rate constants between dissolved compounds and $^{3}$CBBP*, which could be used to derive estimates of the reactivity between CECs and $^{3}$CDOM* (Minella et al., 2018). Therefore, the goal of the present work is to use CBBP as proxy molecule for the re-assessment of the triplet-sensitisation reactivity of some compounds, for which at the moment only reactivity data with $^{3}$AQ2S* are available. The chosen molecules are acetaminophen, clofibric acid and ibuprofen, for which the $^{3}$AQ2S* reactivity data suggest that the $^{3}$CDOM* reactions may be very important in environmental photodegradation (Vione et al., 2011; De Laurentiis et al., 2014; Avetta et al., 2016). We also studied atrazine, because for this compound an estimate is available of the second-order reaction rate constant with actual $^{3}$CDOM* (Zeng and Arnold, 2013). The study of the reactivity of atrazine with $^{3}$CBBP*, may thus provide further insight into the suitability of CBBP as proxy molecule to assess $^{3}$CDOM* reactivity.

## Materials and Methods

**Reagents and materials.** 4-Carboxybenzophenone (CBBP, purity grade 99%), ibuprofen sodium salt (IBP, 98%), paracetamol (APAP, BioXtra, > 99%), clofibric acid (CLO, 97%), atrazine (ATZ, Pestanal® analytical standard, 98.8%), 2-nitrobenzaldehyde (2-NBA, 98%), $H_3PO_4$ (85%), NaOH (98%) and phenol (99%) were purchased from Aldrich. Methanol (HPLC gradient grade) was purchased from VWR Chemicals BDH. Aqueous solutions were prepared using ultra-pure water, obtained from a Millipore Milli-Q system (resistivity > 18 MΩ cm, organic carbon < 2ppb).

**Irradiation experiments.** The aqueous solutions containing each compound alone (IBP, APAP, CLO, or ATZ) for the direct photolysis (blank) experiments, or binary mixtures of CBBP with each of the studied compounds, were adjusted to pH 7 with NaOH. The pH measurements were carried out by using a combined glass electrode connected to a Metrohm 602 pH meter, calibrated periodically with standard buffers at pH = 4.01, 7.00 and 10.00 (Fluka). In the case of ATZ, limited water solubility prevented preparation of the stock solution by direct weighting. Therefore, an aliquot of solid ATZ was stirred overnight in water, the suspension was filtered on 0.45 μm pore size polyamide filters (Sartorius), and the concentration of the filtered solution was measured by liquid chromatography (*vide infra*) against methanol/water standards.

Solutions to be irradiated (5 mL volume) were placed inside cylindrical Pyrex glass cells (4.0 cm diameter, 2.4 cm height) having a lateral neck for sample transfer, which was kept tightly closed with a screw cap upon irradiation. The optical path length within the irradiated solutions was $b$ = 0.4 cm. The solutions were magnetically stirred during irradiation.

Irradiation took place under an 18W Philips TL-D UVA black lamp, with emission maximum at 369 nm. The UV irradiance ($\lambda \leq 400$ nm) of the lamp on top of the solutions was 40.5 ± 2.5 W $m^{-2}$, corresponding to an incident photon flux of $(3.14 \pm 0.04) \times 10^{-5}$ Einstein $L^{-1}$ $s^{-1}$. The irradiance was measured with a meter by CO.FO.ME.GRA. (Milan, Italy), equipped with a UV-sensitive probe.

The emission spectrum of the lamp was determined by combining spectral measurements with an Ocean Optics USB 2000 CCD spectrophotometer (calibrated in photon flux with an Ocean Optics DH-2000-CAL source), with chemical actinometry based on 2-NBA. The lamp spectrum is reported in **Figure 1**, along with the absorption spectra (molar absorption coefficients) of CBBP, APAP, IBP, CLO and ATZ (note that CLO does not absorb radiation above 300 nm).

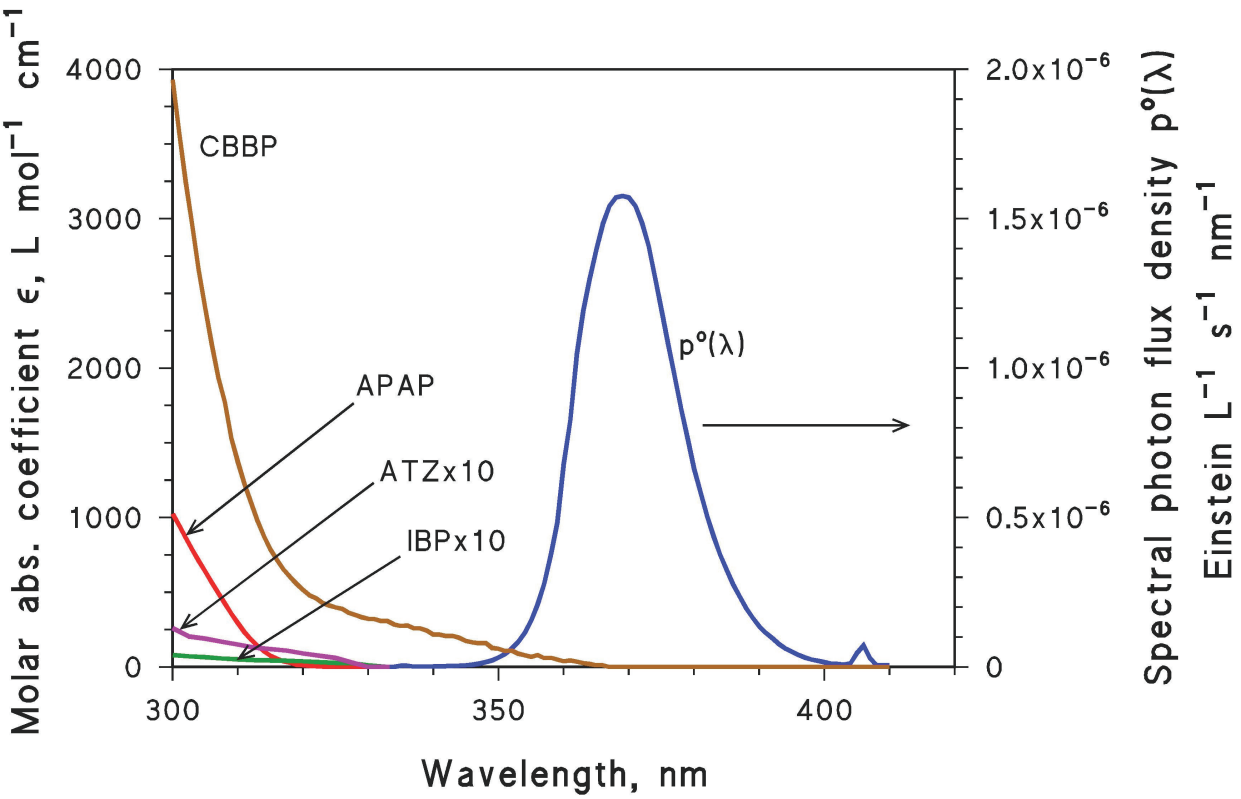


**Figure 1.** *Right Y-axis.* Emission spectrum (incident spectral photon flux density $p°(\lambda)$ in Einstein $L^{-1}$ $nm^{-1}$ $s^{-1}$ units) of the UVA lamp (40.5 ± 2.5 W $m^{-2}$) used for the irradiation experiments. *Left Y-axis.* Absorption spectra (molar extinction coefficients $\varepsilon(\lambda)$) of CBBP, APAP, ATZ and IBP. Note that $\varepsilon_{IBP}(\lambda)$ and $\varepsilon_{ATZ}(\lambda)$ were multiplied by 10 for plot readability issues. Furthermore, CLO does not absorb radiation above 300 nm.

Chemical actinometry exploited the photoisomerisation reaction of 2-NBA into 2-nitrosobenzoic acid. Several $10^{-4}$ mol $L^{-1}$ solutions of 2-NBA were irradiated for up to 3.5 min, to measure the degradation rate of the actinometer ($R_{2\text{-NBA}}$) and determine its absorbed photon flux ($P_a$), based on the known photolysis quantum yield ($\Phi_{2\text{-NBA}} = 0.4$; Allen et al., 2000): $P_a = R_{2\text{-NBA}} (\Phi_{2\text{-NBA}})^{-1}$. Assume $i°(\lambda)$ as the lamp spectrum (in arbitrary units proportional to the photon count) obtained with the CCD spectrophotometer, and $\theta$ as a conversion factor so that the incident spectral photon flux density of the lamp (units of Einstein $L^{-1}$ $s^{-1}$) is $p°(\lambda) = \theta\ i°(\lambda)$. The conversion factor $\theta$ can be obtained as follows:

$$\theta = \frac{R_{2-NBA}}{\Phi_{2-NBA}\int_{\lambda} i^{o}(\lambda)[1-10^{-\varepsilon_{2-NBA}(\lambda)\,b\,C_{2-NBA}}]\,d\lambda} \qquad (1)$$

where $\varepsilon_{2\text{-NBA}}$ is the molar absorption coefficient of 2-NBA, $b = 0.4$ cm, and $C_{2\text{-NBA}} = 10^{-4}$ mol $L^{-1}$.

**Analytical determinations.** The absorption spectra of the irradiated compounds (CBBP, IBU, APAP, CLO, ATZ) were measured with a Varian Cary 100 Scan double-beam, UV-Vis spectrophotometer, using Hellma quartz cuvettes with 1 cm optical path length. The time trends of APAP, IBU, CLO and ATZ were monitored by high-performance liquid chromatography coupled with diode array detection (HPLC-DAD). The used LaChrom Elite instrument (VWR-Hitachi) was equipped with a L-2200 Autosampler (injection volume 60 µL), a L-2130 quaternary pump for low-pressure gradients, a L-2300 column oven (set at 40 °C), and a L-2455 DAD detector. The column was a RP-C18 LichroCART (VWR Int., length 125 mm, diameter 4 mm), packed with LiChrospher 100 RP-18 (5 µm diameter). The different compounds were eluted in either isocratic or gradient mode, with a mixture of A = 5.7 mmol $L^{-1}$ $H_3PO_4$ in water (pH ~ 3) and B = methanol, at a flow

rate of 1 mL $min^{-1}$ (the column dead time was 1.5 min). The following conditions were used (λ = detection wavelength, $t_R$ = retention time) in the different systems:

*(i)* CBBP + APAP. Gradient elution (10% B for 4 min, up to 70% B in 1.5 min, keep for 4 min, down to 10% B in 2 min, keep for 4.5 min); CBBP (λ = 262 nm, $t_R$ = 9.9 min); APAP (λ = 245 nm, $t_R$ = 4.8 min).

*(ii)* CBBP + IBP. Isocratic elution (37.5% A, 62.5% B); CBBP (λ = 262 nm, $t_R$ = 11.3 min); IBP (λ = 220 nm, $t_R$ = 4.0 min).

*(iii)* CBBP + CLO. Gradient elution (30% B for 4 min, up to 55% B in 0.1 min, keep for 10.9 min, down to 30% B in 0.1 min, keep for 1.9 min); CBBP (λ = 262 nm, $t_R$ = 12.1 min); CLO (λ = 227 nm, $t_R$ = 12.8 min).

*(iv)* CBBP + ATZ. Isocratic elution (60% A, 40% B); CBBP (λ = 262 nm, $t_R$ = 27.3 min); ATZ (λ = 220 nm, $t_R$ = 19.8 min).

**Laser flash photolysis (LFP) experiments.** The quenching kinetics of $^3$CBBP* by the studied substrates was assessed using the third harmonic (355 nm) of a Quanta Ray GCR 130-01 Nd:YAG laser system instrument, used in a right-angle geometry with respect to the monitoring light beam. The single pulses energy was set to 35-40 mJ. A 3 mL solution volume containing 100 μmol $L^{-1}$ CBBP in water at pH ~7 was placed into a quartz cuvette (path length of 1 cm), and used for a maximum of four consecutive laser shots. Where applicable, the solution also contained variable concentrations of $^3$CBBP* quenchers (ATZ, APAP, IBP). The absorbance of $^3$CBBP* at 340 (ATZ, IBP) or 480 nm (APAP) was monitored over time by a detection system consisting of a pulsed xenon lamp (150 W), monochromator and a photomultiplier (1P28). A spectrometer control unit was used for synchronising the pulsed light source and programmable shutters with the laser output. The signal from the photomultiplier was digitised by a programmable digital oscilloscope

(HP54522A). A 32 bits RISC-processor kinetic spectrometer workstation was used to analyse the digitised signal.

The decay of $^3$CBBP* was monitored at different concentration values of the added quenchers, and the measured pseudo-first order decay constant $k_{^3CBBP^*}$ was reported as a function of the quencher concentration. The slopes of the linearly fitted data of $k_{^3CBBP^*}$ vs. [Quencher] give the second-order quenching rate constants of $^3$CBBP* by ATZ, APAP and IBP (Stern-Volmer approach).

**Kinetic data treatment.** The irradiated substrates in the presence of CBBP underwent degradation following pseudo-first order kinetics, thus the relevant time trends were fitted with the equation $C_t = C_o\, e^{-k\, t}$, where $C_t$ is the substrate concentration at the time $t$, $C_o$ the initial concentration, and $k$ the pseudo-first order degradation rate constant. The initial degradation rate is derived as $R_o = k\, C_o$.

In experimental series where $C_o$ is varied, the plot of $R_o$ vs. $C_o$ should give a straight line (i.e., the value of $k$ should be independent of $C_o$) for sufficiently low $C_o$ values (Minella et al., 2018). Assume $m$ as the slope of the line $R_o$ vs. $C_o$, and S as the substrate undergoing irradiation in the presence of CBBP. The second-order reaction rate constant between S and CBBP can be obtained as follows (Minella et al., 2018):

$$k_{S,^3CBBP^*} = k'\left(\frac{m}{P_{a,CBBP}} - \frac{0.68\, S_\Delta\, k_{^1O_2,S}}{k''}\right) \qquad (2)$$

where $k' = 6\times10^5$ s$^{-1}$ is the first-order deactivation rate constant of $^3$CBBP* in aerated solution, 0.68 is the fraction of $^3$CBBP* quenched by $O_2$ in aerated solution, $S_\Delta = 0.46$ is the $^1O_2$ yield upon interaction between $^3$CBBP* and $O_2$ (which means that quenching of $^3$CBBP* by $O_2$ yields CBBP + $^1O_2$ in the 46% of cases, and CBBP + $O_2$ in the remaining 54%), $k_{^1O_2,S}$ is the reaction rate constant between S and $^1O_2$, $k'' = 2.5\times10^5$ s$^{-1}$ is the quenching rate constant of $^1O_2$ upon collision with the

water solvent, and $P_{a,CBBP}$ is the photon flux absorbed by CBBP (Minella et al., 2018). Note that for the studied substrates S = APAP, CLO, ATZ and IBP, the $^1O_2$ reaction rate constants $k_{^1O_2,S}$ are available in the literature (Vione et al., 2011; Marchetti et al., 2013; De Laurentiis et al., 2014; Avetta et al., 2016).

It is interesting to observe that **Eq. (2)** in the reported linearised form is valid only if $k_{S,^3CBBP^*}$ [S] « $k'$ and $k_{^1O_2,S}$ [S] « $k''$, where [S] is the substrate concentration (Minella et al., 2018). The highest values of [S] used experimentally were in the order of $10^{-4}$ mol $L^{-1}$, thus $k_{^1O_2,S}$ [S] would be in the range of $4\times10^0$-$4\times10^3$ $s^{-1}$ depending on the compound, and thus always much lower than $k''$. On the other hand, $k_{S,^3CBBP^*}$ [S] « $k'$ implies that $k_{S,^3CBBP^*}$ « $6\times10^9$ L $mol^{-1}$ $s^{-1}$. This condition was actually not met for all the compounds (*vide infra*), thus in some cases it was necessary to use only the experimental data obtained at the lowest [S] values for the determination of $k_{S,^3CBBP^*}$.

Because we used the studied compounds at low concentration, CBBP was the main radiation absorber in solution, i.e., it was $\varepsilon_{CBBP}(\lambda)[CBBP] \gg \varepsilon_S(\lambda)[S]$, where $\varepsilon_{CBBP}(\lambda)$ is the molar absorption coefficient of CBBP, [CBBP] its molar concentration (70 μmol $L^{-1}$ in all the experiments), $\varepsilon_S(\lambda)$ the molar absorption coefficient of S, and [S] its molar concentration. In this case, $P_{a,CBBP}$ can be calculated as follows (Braslavky, 2007):

$$P_{a,CBBP} = \int_{\lambda} p°(\lambda)\ (1-10^{-b(\varepsilon_{CBBP}(\lambda)[CBBP])})\, d\lambda \qquad (3)$$

where $p°(\lambda)$ is the incident spectral photon flux density in the irradiated solution, and $b$ = 0.4 cm is the optical path length (see **Figure 1** for $p°(\lambda)$ and $\varepsilon_{CBBP}(\lambda)$).

An interesting issue with the $^3$CDOM*-mediated processes is that they often entail one-electron oxidation of (or H-atom abstraction from) dissolved substrates (Canonica and Laubscher, 2008;

Wenk and Canonica, 2012; Janssen et al., 2014; Leresche et al., 2016). The oxidised reaction intermediates (e.g., radicals or radical cations) may evolve into transformation products, but in some cases the phenolic moieties occurring in the natural dissolved organic matter are able to reduce the oxidised intermediates back to the parent compounds. This back-reduction effect has been actually observed with some CECs. The effect can be kinetically treated, by assuming that the degradation rate constant $k_o$ observed in the absence of antioxidants is decreased by a factor $\psi < 1$ in the presence of organic compounds with reductive capabilities (i.e., $k = k_o\ \psi$) (Canonica and Laubscher, 2008; Wenk and Canonica, 2012).

Phenol can be used as model reductant to study the back-reduction effect, and the functional form of $\psi$ as a function of phenol concentration has two possible expressions (Wenk et al., 2011; Wenk and Canonica, 2013):

$$\psi = \frac{1}{1 + \frac{[PhOH]}{[PhOH]_{1/2}}} \tag{4}$$

$$\psi = \frac{f}{1 + \frac{[PhOH]}{[PhOH]_{1/2}}} + (1 - f) \tag{5}$$

where [PhOH] is the molar concentration of added phenol and, in the case of **Eq. (4)**, $[PhOH]_{1/2}$ is the concentration of phenol that causes $k$ to be halved compared to $k_o$ ($\psi = 0.5$). In the case of **Eq. (5)**, $[PhOH]_{1/2}$ is the concentration of phenol that gives $\psi = 1 - f/2$. The trend described by **Eq. (4)** is observed when phenol reduces all the intermediate radicals produced by triplet-sensitised oxidation (one reaction channel), while the trend described by **Eq. (5)** is observed when phenol reduces only a fraction of such radicals (two parallel reaction channels) (Wenk et al., 2011; Wenk and Canonica, 2013). Indeed, **Eq. (4)** can be obtained from **Eq. (5)** when $f = 1$.

**Modelling of environmental photochemistry.** To get insight into the environmental significance of the measured $k_{S,^3CBBP^*}$ values, we carried out photochemical modelling of substrate photodegradation in environmental surface waters by using the APEX software (Aqueous Photochemistry of Environmentally-occurring Xenobiotics, available for free as Electronic Supplementary Information of Bodrato and Vione, 2014). APEX predicts photochemical reaction kinetics (i.e., first-order photodegradation rate constants and half-life times) from photoreactivity parameters (absorption spectra, direct photolysis quantum yields and second-order reaction rate constants with transient species) and from data of water chemistry and depth (Bodrato and Vione, 2014; Vione, 2014). APEX predictions have been validated by comparison with field data of pollutant phototransformation kinetics in surface freshwaters. In the present case we used APEX to compare the measured $k_{S,^3CBBP^*}$ values with the literature data concerning $k_{S,^3AQ2S^*}$ (i.e., the second-order reaction rate constant between the substrate S and the AQ2S triplet state), as estimates of $k_{S,^3CDOM^*}$. The latter represents the second-order reaction rate constant between S and $^3$CDOM*. The overall goal was to assess the differences in the predicted environmental importance of the $^3$CDOM* reactions for each relevant compound, obtained by using either AQ2S or CBBP as CDOM proxy (i.e., by using either $k_{S,^3AQ2S^*}$ or $k_{S,^3CBBP^*}$ as $k_{S,^3CDOM^*}$ estimate).

The APEX software computes the absorption of radiation by the photosensitisers (CDOM, nitrate and nitrite) and the studied substrates by considering competition for sunlight irradiance. Calculations are carried out in the framework of a Lambert-Beer approach (Bodrato and Vione, 2014; Braslavsky, 2007). APEX applies to well-mixed waters and gives average values over the water column, which includes the contributions of the well-illuminated surface layer and of darker water in the lower depths, where irradiance is very low (Loiselle et al., 2008). The time unit of the standard output is fair-weather days equivalent to 15 July at 45°N latitude (the functions to determine seasonal variations of photoreactivity were not used in this work).

## Results and Discussion

The studied compounds (APAP, IBP, CLO and ATZ) did not undergo significant direct photolysis under irradiation, because they do not absorb lamp radiation significantly (see **Figure 1**). Their time trends under irradiation in the presence of CBBP are reported in the Supplementary Material (hereinafter, SM), **Figure SM1**. All compounds followed pseudo-first order photodegradation kinetics, and linear trends of $R_S$ vs. [S] (S = APAP, IBP, CLO or ATZ) were observed up to [S] = $10^{-4}$ mol $L^{-1}$ (100 µmol $L^{-1}$) for IBP and CLO, and up to around 20 µmol $L^{-1}$ for APAP and ATZ (higher ATZ concentrations were not used because of solubilisation issues) (**Figure 2**). The linear part of the trends allowed for the calculation of $k_{S,^3CBBP^*}$ by using **Eqs. (2,3)** (see **Table 1** for the $k_{S,^3CBBP^*}$ data). It is interesting to observe that the first-order degradation rate constants $k$ of the studied substrates S decreased when increasing the initial concentration [S], as expected (see **Figure SM1**). There was the exception of ATZ, where $k$ was poorly dependent on [S] but where relatively low values of [S] were used. The reason for $R_S = k \times [S]$ to be reasonably linearly dependent on [S], despite the fact that $k$ was not constant, is that the variation ranges of $k$ and [S] were rather different. Indeed, $k$ varied by a factor of 1.6 (APAP, only the linear portion considered), 1.7 (IBP), or 2 (CLO, ATZ), while at the same time the [S] variation factor was as large as 4.2 (APAP), 7.5 (ATZ), 25 (CLO), and 28 times (IBP). Therefore, the important [S] variations overcame those of $k$ to produce the observed, practically linear trends.

It is also interesting to compare the values of $k_{S,^3CBBP^*}$ reported in **Table 1** with the quenching rate constants $k^Q_{S,^3CBBP^*}$ obtained with the LFP technique. We got $k^Q_{ATZ,^3CBBP^*} = 1.2\times10^9$ L $mol^{-1}$ $s^{-1}$, $k^Q_{APAP,^3CBBP^*} = 2.5\times10^9$ L $mol^{-1}$ $s^{-1}$, and $k^Q_{IBP,^3CBBP^*} = 1.5\times10^9$ L $mol^{-1}$ $s^{-1}$. One has $k^Q_{S,^3CBBP^*} \geq k_{S,^3CBBP^*}$, in agreement with the fact that the quenching rate constants $k^Q_{S,^3CBBP^*}$ account both for physical quenching, and for the chemical reactivity between S and $^3$CBBP*.

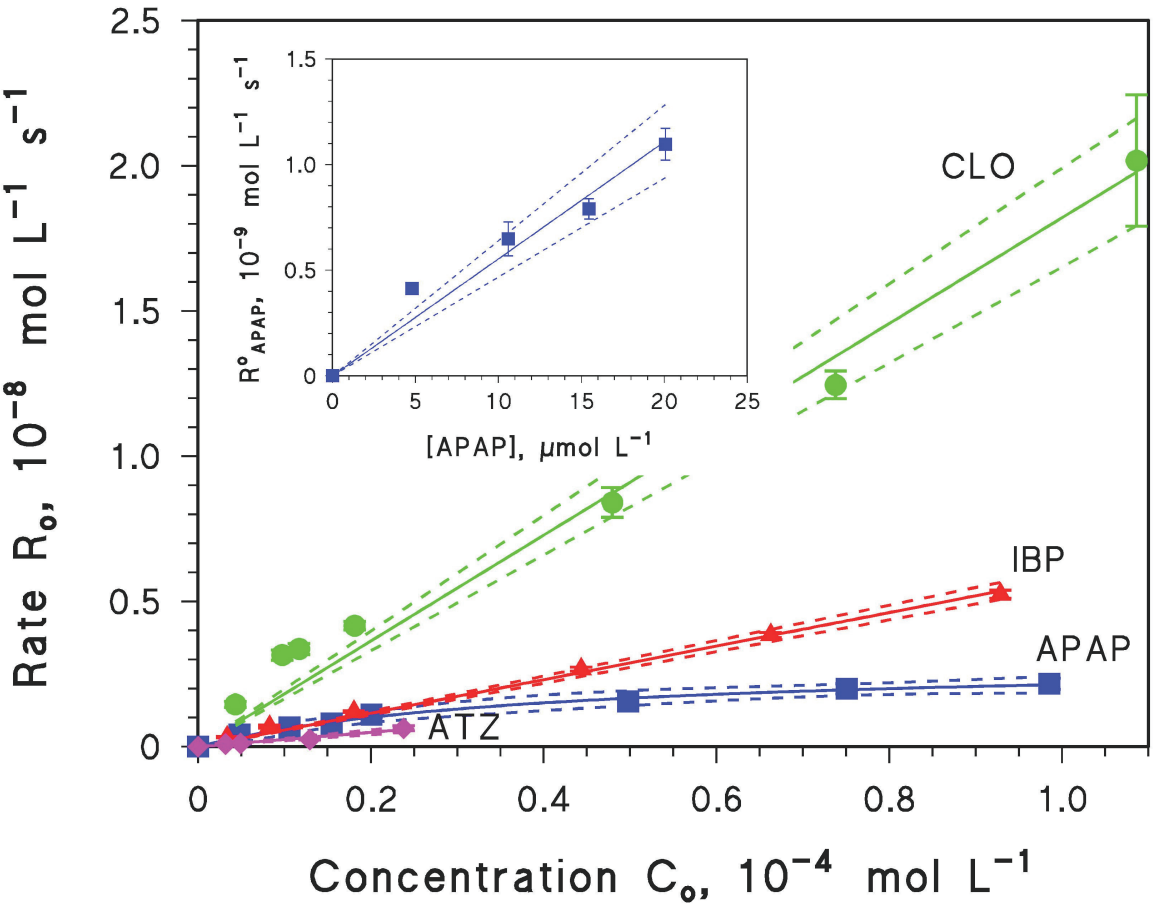


**Figure 2.** Trends of the initial degradation rates $R_o$ of the studied substrates (APAP, IBP, CLO and ATZ) as a function of the initial substrate concentration ($C_o$). The time trends of **Figure SM1** were fitted with exponential equations of the form $C_t = C_o\, e^{-k\,t}$, where $C_t$ is the concentration of the substrate at the time $t$ and $k$ is the pseudo-first order photodegradation rate constant. The initial rates were calculated as $R_o = k\, C_o$. The error bars on the figure represent the sigma-level uncertainty on the determination of $k$ by numerical fit. The solid curves represent the fit of the $R_o$ vs. $C_o$ data, while the dashed ones are the 95% confidence limits of the fit. The linear trend of $R_o$ vs. $C_o$, observed in most cases, is due to the fact that $k$ has limited dependence on $C_o$. The figure insert shows the linear portion of the $R_o$ vs. $C_o$ plot in the case of APAP.

**Table 1.** Comparison between the literature second-order rate constants for the reaction of the studied compounds with $^3$AQ2S*, and the second-order rate constants obtained in this work for $^3$CBBP*. The $\psi$ function that describes the back-reduction process is also reported ($\psi$ = 1 means that no back reduction was observed). The $DOC_{1/2}$ value was obtained from the experimental $[PhOH]_{1/2}$ value, by assuming $DOC_{1/2}$ [$mg_C$ $L^{-1}$] = 0.4 $[PhOH]_{1/2}$ [μmol $L^{-1}$] as per previous work (Vione et al., 2018). n/a = not applicable. The error bounds represent the sigma-level uncertainty, derived from the linear data fit of $R_S$ vs. [S].

| **Compound, S** | $k_{S,^3AQ2S^*}$, **L mol$^{-1}$ s$^{-1}$** | $k_{S,^3CBBP^*}$, **L mol$^{-1}$ s$^{-1}$** | $\psi$ | **$DOC_{1/2}$, $mg_C$ L$^{-1}$** | $f$ |
|---|---|---|---|---|---|
| **APAP** | $(1.08\pm0.16)\times10^{10}$ ***(a)*** | $(1.59\pm0.09)\times10^{9}$ | 1 | n/a | n/a |
| **IBP** | $(9.7\pm0.2)\times10^{9}$ ***(b)*** | $(1.53\pm0.02)\times10^{9}$ | 1 | n/a | n/a |
| **CLO** | $(1.2\pm0.1)\times10^{10}$ ***(c)*** | $(5.23\pm0.20)\times10^{9}$ | $\frac{f}{1+\frac{DOC}{DOC_{1/2}}}+(1-f)$ | 0.1 | 0.32 |
| **ATZ** | $(1.43\pm0.07)\times10^{9}$ ***(d)*** | $(7.15\pm0.43)\times10^{8}$ | 1 | n/a | n/a |

***(a)*** De Laurentiis et al., 2014. ***(b)*** Vione et al., 2011.
***(c)*** Avetta et al., 2016. ***(d)*** Marchetti et al., 2013.

**Table 1** summarises the second-order reaction rate constants of the studied compounds with $^3$AQ2S* ($k_{S,^3AQ2S^*}$) as available in the literature, and compares them with the $^3$CBBP* reaction rate constants obtained in this work ($k_{S,^3CBBP^*}$). The comparison between $k_{S,^3AQ2S^*}$ and $k_{S,^3CBBP^*}$ shows that, first of all, the $^3$CBBP* reaction rate constants are consistently lower that those with $^3$AQ2S*. This finding is coherent with the fact that the $^3$CBBP* one-electron reduction potential ($E^o_{^3CBBP^*/CBBP^{\bullet-}}$ = 1.8 V) is quite below that of $^3$AQ2S* ($E^o_{^3AQ2S^*/AQ2S^{\bullet-}}$ = 2.6 V) (McNeill and Canonica, 2016). Moreover, the $k_{S,^3AQ2S^*}$ values in the cases of APAP, IBP and CLO are quite near the diffusive control limit in aqueous solution, and they are a bit too high to represent typical $k_{S,^3CDOM^*}$ values. Actually, there is evidence that the latter have an upper limit of around $5\times10^9$ L mol$^{-1}$ s$^{-1}$ (Canonica et al., 2000).

In the case of CLO the value of $k_{S,^3CBBP*}$ is near the $k_{S,^3CDOM*}$ upper limit, but this issue is compensated for by the fact that $\psi < 1$. Indeed, phenol as model antioxidant significantly inhibited the CBBP-induced photodegradation of CLO, while phenol had practically negligible effects in all the other cases under study (**Figure SM2**). The trend of $\psi = R_{CLO}/R^{\circ}_{CLO}$ (ratio between the initial degradation rates of CLO in the presence and in the absence of phenol) vs. [Phenol] was fitted with **Eq. (5)**. In order to take the CLO back-reduction effect into account, when using the $^3$CBBP* data ($k_{CLO,^3CBBP*}$) to model the $^3$CDOM* reaction, one has to assume $k_{CLO,^3CDOM*} = \psi k_{CLO,^3CBBP*}$, in analogy with previous studies on different substrates (Vione et al., 2018).

In the case of IBP, there is evidence that the $k_{IBP,^3AQ2S*}$ value leads to overestimations of photodegradation kinetics with $^3$CDOM* (Vione et al., 2011; Packer et al., 2003; Tixier et al., 2003). Moreover, the experimental observations that $^{\bullet}$OH and direct photolysis are not the only IBP phototransformation pathways (Packer et al., 2003), and that IBP is efficiently photodegraded by irradiated fulvic acids (Jacobs et al., 2011), suggest that $k_{IBP,^3CDOM*}$ should be at least $10^8$ L mol$^{-1}$ s$^{-1}$, and most likely quite higher than that (Vione et al., 2011). However, $k_{IBP,^3CDOM*}$ should be lower than $k_{IBP,^3AQ2S*} = (9.7\pm0.2)\times10^9$ L mol$^{-1}$ s$^{-1}$. On this basis, our value of $k_{IBP,^3CBBP*} = (1.53\pm0.02)\times10^9$ L mol$^{-1}$ s$^{-1}$ looks like a reasonable estimate of $k_{IBP,^3CDOM*}$.

The case of ATZ is very interesting because for this compound there is an independent estimate of the $^3$CDOM* rate constant. While the $k_{S,^3CDOM*}$ values may vary depending on the CDOM type, they still make a valuable reference to compare with the corresponding proxy data. The available value of $k_{ATZ,^3CDOM*}$ ($1.2\times10^9$ L mol$^{-1}$ s$^{-1}$; Zeng and Arnold, 2013) is quite closely bracketed by those of $k_{ATZ,^3AQ2S*}$ ($1.4\times10^9$ L mol$^{-1}$ s$^{-1}$) and $k_{ATZ,^3CBBP*}$ ($0.7\times10^9$ L mol$^{-1}$ s$^{-1}$) (**Table 1**). This means that both AQ2S and CBBP provide a reasonable estimate of $^3$CDOM* reactivity in the case of ATZ.

ATZ is one of the instances in which the AQ2S-based value is proven to be reliable, but the CBBP estimate for $k_{ATZ,^3CDOM*}$ is also suitable. However, in other cases there is evidence that $^3$CBBP* is a better indicator of $^3$CDOM* reactivity than $^3$AQ2S*. This means that the $k_{S,^3CBBP*}$ values may allow for better prediction of photochemical lifetimes in the field compared to $k_{S,^3AQ2S*}$, as in the case of naproxen (Avetta et al., 2016).

The available data from the literature and this work suggest that CBBP may be a viable proxy molecule to assess the reactivity of $^3$CDOM*. It is then interesting to compare the environmental importance of the $^3$CDOM* reactions obtained from previous, AQ2S-based estimates, with the new data based on $^3$CBBP* reactivity and (where applicable) the back-reduction process. In other words, by use of photochemical modelling, comparison is here made between a scenario where $k_{S,^3CDOM*} = k_{S,^3AQ2S*}$ (AQ2S proxy), and a scenario where $k_{S,^3CDOM*} = \psi k_{S,^3CBBP*}$ (CBBP proxy + back-reduction, the latter being important for CLO alone). The additional photoreactivity parameters used for the different compounds in photochemical modelling, namely the direct photolysis quantum yields and the second-order reaction rate constants with $^{\bullet}$OH, $CO_3^{\bullet-}$ and $^1O_2$, are reported in **Table SM1** in the SM (note that the reaction rate constants with $^1O_2$ were also used to determine $k_{S,^3CBBP*}$ with **Eq. (2)**). The model exercise was carried out for two different environmental contexts, namely a shallow water body (water depth $d$ = 0.5 m) and a deeper one ($d$ = 5 m). The considered DOC range (1-10 $mg_C\ L^{-1}$) is representative of the conditions found in lakes located in temperate areas with a variety of trophic statuses (Wetzel, 2001).

The model results for APAP are reported in **Figure 3**, for $d$ = 0.5 m and AQ2S proxy **(3a)**, $d$ = 0.5 m and CBBP proxy **(3b)**, $d$ = 5 m and AQ2S proxy **(3c)**, as well as $d$ = 5 m and CBBP proxy **(3d)**. The comparison of the AQ2S- and CBBP-based scenarios clearly shows that in the second case one has a considerably lower importance of the $^3$CDOM* reactions, coherently with the fact that $k_{APAP,^3CBBP*} \sim 0.15\ k_{APAP,^3AQ2S*}$ ($\psi$ = 1). Differences between the two scenarios are quite limited at

low DOC, where direct photolysis and $CO_3^{\bullet-}$ reactions would play very important roles in APAP photodegradation. Not surprisingly, differences become important at high DOC that favours $^3$CDOM*. However, even in the CBBP-proxy scenario, degradation by $^3$CDOM* would still dominate the phototransformation of APAP at high DOC. The main difference between the AQ2S and CBBP scenarios lies in the photochemical lifetimes in DOM-rich waters, which are considerably higher in the case of CBBP. Indeed, the modelled APAP lifetimes at high DOC increase from ~ 1 day to ~ 1 week ($d$ = 0.5 m), and from ~ 1 to ~ 3 weeks ($d$ = 5 m) when passing, respectively, from the AQ2S to the CBBP proxy. By the way, lifetimes are always longer in deeper waters because these combine a well-irradiated surface layer with darker lower depths. Actually, the deep water-bodies are more scarcely illuminated by sunlight, on average, compared to shallow aqueous environments.

The importance of the $^3$CDOM* processes is a bit higher in deep than in shallow water, because CDOM (the $^3$CDOM* source) absorbs both UV and visible radiation. In contrast, APAP direct photolysis and the photochemistry of nitrate and nitrite (direct $^{\bullet}$OH and indirect $CO_3^{\bullet-}$ sources) are triggered by UV radiation only, which shows much shallower penetration into water columns compared to visible light (Loiselle et al., 2008; Tartarotti et al., 2017).

Model results for IBP are reported in **Figure SM3**, for the same scenarios already seen with APAP. Interestingly, in this case the lower reactivity predicted for $^3$CDOM* by using CBBP instead of AQ2S, prevents the $^3$CDOM* reaction to become the main IBP phototransformation process, at DOC values around 10 $mg_C\ L^{-1}$ and $d$ = 0.5 m. In contrast, in both scenarios (AQ2S and CBBP), $^3$CDOM* is still predicted to be the main high-DOC route for IBP photodegradation at $d$ = 5 m. However, for both $d$ = 0.5 m and $d$ = 5 m, one gets 3-4 times slower photodegradation kinetics at high DOC in the CBBP scenario compared to AQ2S.

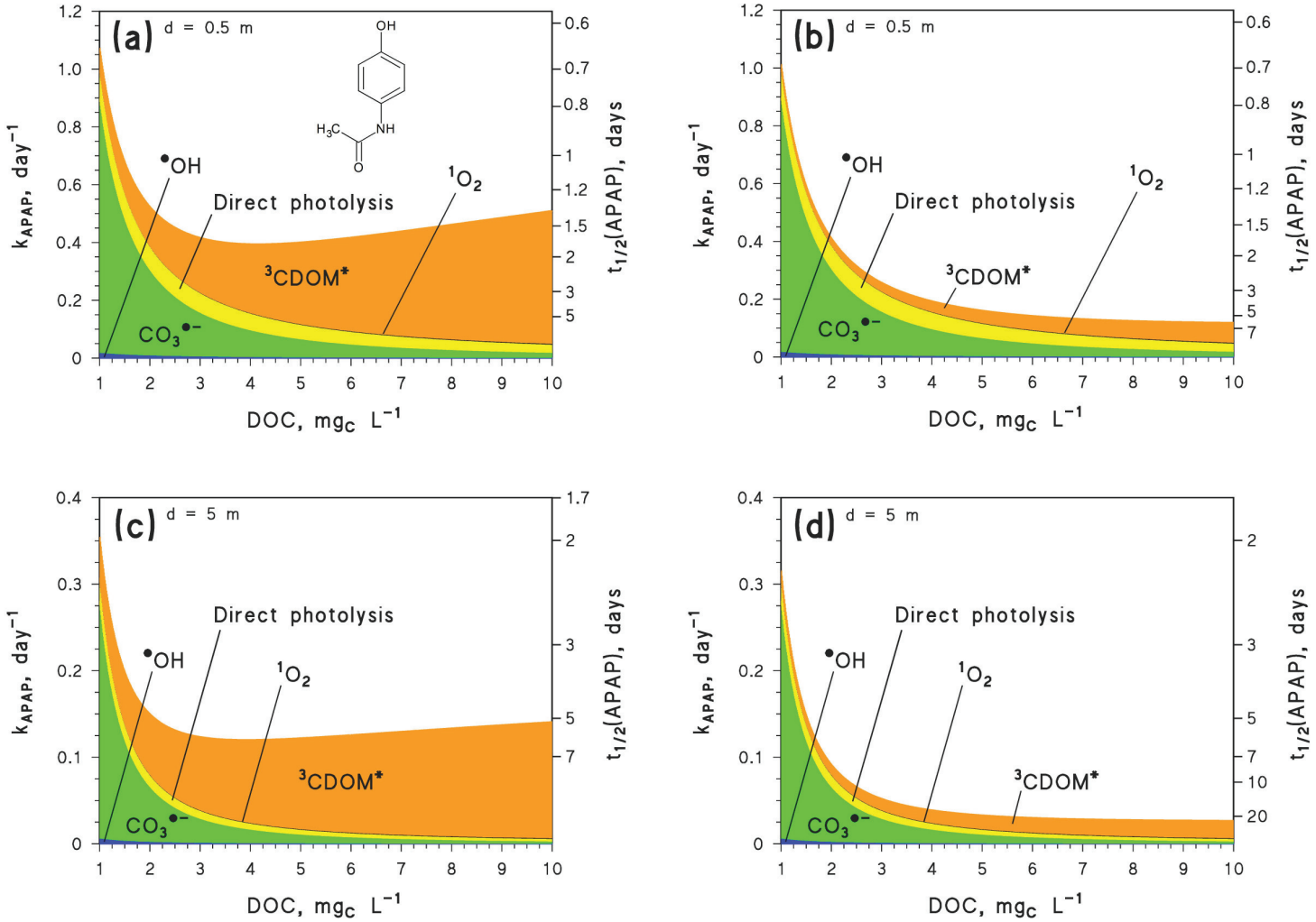


**Figure 3.** Modelled APAP phototransformation kinetics and pathways (left Y-axis: first-order rate constants; right-Y axis: lifetimes; colour codes: pathways) for: **(a)** $d$ = 0.5 m and $k_{S,^3CDOM*} = k_{S,^3AQ2S*}$; **(b)** $d$ = 0.5 m and $k_{S,^3CDOM*} = \psi k_{S,^3CBBP*}$ ($\psi$=1); **(c)** $d$ = 5 m and $k_{S,^3CDOM*} = k_{S,^3AQ2S*}$; **(d)**, $d$ = 5 m and $k_{S,^3CDOM*} = \psi k_{S,^3CBBP*}$. Other water conditions: $10^{-4}$ mol L$^{-1}$ $NO_3^-$, $10^{-6}$ mol L$^{-1}$ $NO_2^-$, $10^{-3}$ mol L$^{-1}$ $HCO_3^-$, $10^{-5}$ mol L$^{-1}$ $CO_3^{2-}$.

The model results for CLO (**Figure 4**), which is practically only degraded by $^{\bullet}$OH and $^3$CDOM*, do not show an abrupt change in the importance of $^3$CDOM* photodegradation at high DOC between the AQ2S-proxy and the CBBP-proxy scenarios. In both cases, $^3$CDOM* would be the prevailing photodegradation pathway at intermediate to high DOC values (in the AQ2S case, however, $^3$CDOM* already prevails at low DOC). Again, the main change is that the predicted lifetimes at DOC ~ 10 $mg_C$ $L^{-1}$ are approximately three times higher in the CBBP case. This effect is a consequence of both $k_{CLO,^3CBBP*} < k_{CLO,^3AQ2S*}$, and of the CLO back-reduction phenomenon that is taken into account by the $\psi$ factor.

In the case of ATZ, where one has $k_{ATZ,^3CBBP*} \sim 0.5\ k_{ATZ,^3AQ2S*}$, the differences between the two scenarios are quite limited (see **Figure SM4**). Although the high-DOC lifetimes at $d$ = 5 m are inversely proportional to the chosen $k_{ATZ,^3CDOM*}$ estimate, differences between CBBP and AQ2S are very small (and practically well within the model uncertainty; Bodrato and Vione, 2014) for $d$ = 0.5 m and high DOC, where $^{\bullet}$OH and the direct photolysis play non-negligible roles in ATZ phototransformation. Therefore, in the ATZ case the differences in the predicted $^3$CDOM* reaction kinetics do not automatically translate into comparable changes in the overall phototransformation.

Interestingly, in all the CBBP-proxy scenarios one needs higher DOC values for the $^3$CDOM* process to overcome the other photoreaction pathways, compared to the case of AQ2S. This issue is quantitatively summarised in **Table 2**.

The modelled photodegradation rate constants and lifetimes allow for a comparison of the predicted AQ2S- and CBBP-based photodegradation kinetics with available field or experimental data. In the case of IBP in lake Greifensee (Switzerland, $10^{-4}$ mol $L^{-1}$ $NO_3^-$, 3.5 $mg_C$ $L^{-1}$ DOC, 2 mmol $L^{-1}$ $HCO_3^-$, $10^{-5}$ mol $L^{-1}$ $CO_3^{2-}$, 5 m epilimnion depth) the photodegradation rate constant should be in the range of 0.006-0.012 $day^{-1}$ during summer (Tixier et al., 2003; Vione et al., 2011). By comparison, AQ2S-based photochemical modelling overestimated $k$ at 0.049±0.017 $day^{-1}$ (μ±σ), while in the CBBP scenario we got $k$ = 0.008±0.003 $day^{-1}$, well within the field-data range.

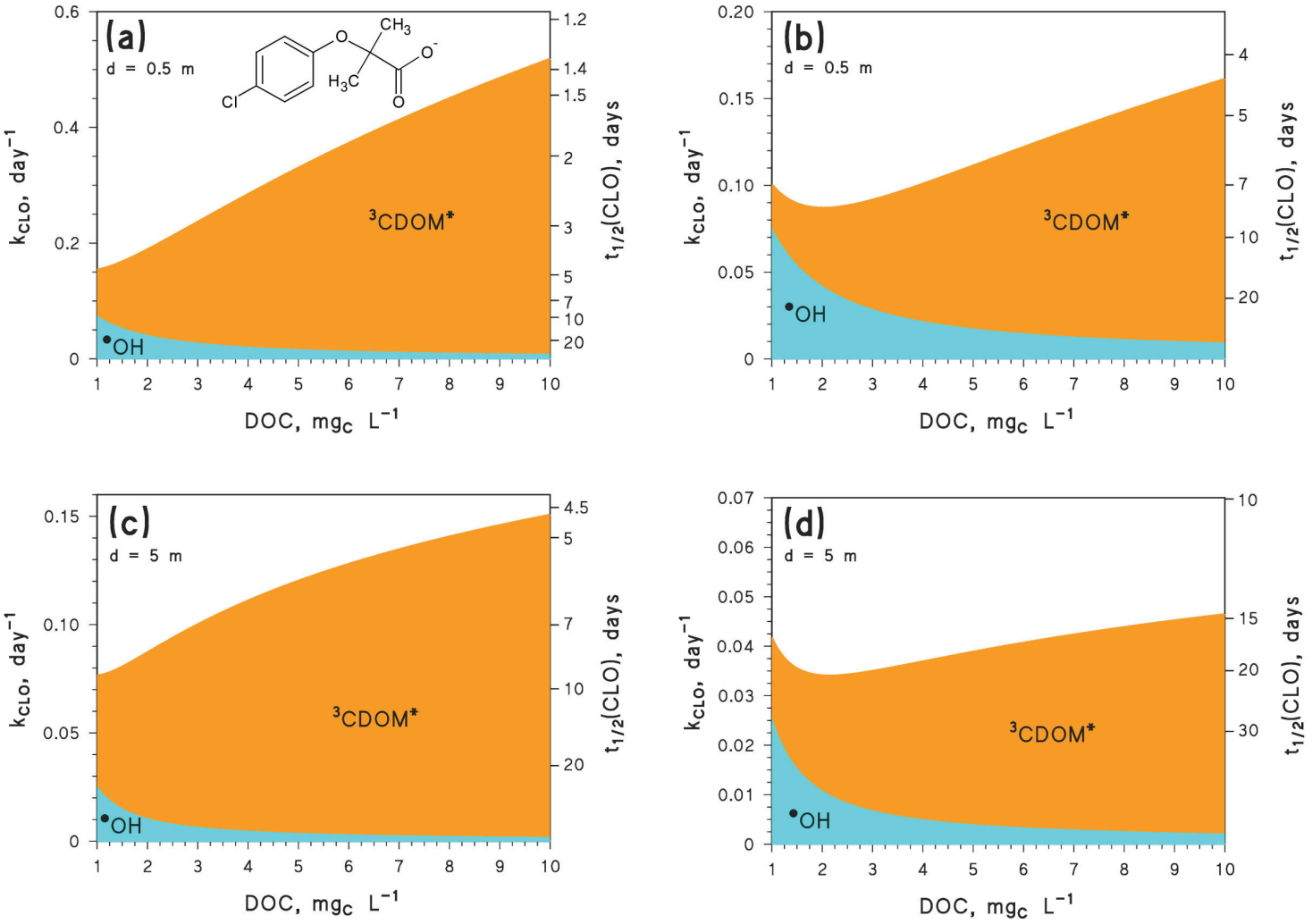


**Figure 4.** Modelled CLO phototransformation kinetics and pathways (left Y-axis: first-order rate constants; right-Y axis: lifetimes; colour codes: pathways) for: **(a)** $d$ = 0.5 m and $k_{S,^3CDOM*} = k_{S,^3AQ2S*}$; **(b)** $d$ = 0.5 m and $k_{S,^3CDOM*} = \psi k_{S,^3CBBP*}$ ($\psi$<1); **(c)** $d$ = 5 m and $k_{S,^3CDOM*} = k_{S,^3AQ2S*}$; **(d)**, $d$ = 5 m and $k_{S,^3CDOM*} = \psi k_{S,^3CBBP*}$. Other water conditions: $10^{-4}$ mol L$^{-1}$ $NO_3^-$, $10^{-6}$ mol L$^{-1}$ $NO_2^-$, $10^{-3}$ mol L$^{-1}$ $HCO_3^-$, $10^{-5}$ mol L$^{-1}$ $CO_3^{2-}$.

**Table 2.** Outline of the DOC values for which the $^3$CDOM* process prevails over the other phototransformation pathways for the considered compound (S = APAP, IBP, CLO or ATZ), in different scenarios (AQ2S proxy, $k_{S,^3CDOM*} = k_{S,^3AQ2S*}$, vs. CBBP proxy, $k_{S,^3CDOM*} = \psi k_{S,^3CBBP*}$; $d$ = 0.5 m vs. $d$ = 5 m). The mentioned "DOC range" is the 1-10 $mg_C\ L^{-1}$ interval used in photochemical modelling.

| Compound, S | AQ2S proxy | CBBP proxy |
|---|---|---|
| | $^3$CDOM* prevalence for $d$ = 0.5 m | |
| APAP | DOC > 3 $mg_C\ L^{-1}$ | DOC > 8 $mg_C\ L^{-1}$ |
| IBP | DOC > 4 $mg_C\ L^{-1}$ | Never in DOC range |
| CLO | Always in DOC range | DOC > 2 $mg_C\ L^{-1}$ |
| ATZ | DOC > 3 $mg_C\ L^{-1}$ | DOC > 5 $mg_C\ L^{-1}$ |
| | $^3$CDOM* prevalence for $d$ = 5 m | |
| APAP | DOC > 2 $mg_C\ L^{-1}$ | DOC > 5 $mg_C\ L^{-1}$ |
| IBP | DOC > 2 $mg_C\ L^{-1}$ | DOC > 8 $mg_C\ L^{-1}$ |
| CLO | Always in DOC range | DOC > 1.5 $mg_C\ L^{-1}$ |
| ATZ | DOC > 2 $mg_C\ L^{-1}$ | DOC > 3 $mg_C\ L^{-1}$ |

Laboratory irradiation of IBP in Mississippi river water (63 µmol $L^{-1}$ $NO_3^-$, 8.9 $mg_C\ L^{-1}$ DOC, 2.5 cm optical path length) yielded $k_{exp}$ = 0.09 $day^{-1}$ (Packer et al., 2003), to be compared with the model predictions $k_{APEX}$ = 0.31±0.11 $day^{-1}$ (AQ2S) and $k_{APEX}$ = 0.055±0.020 $day^{-1}$ (CBBP). In the case of CLO, again in lake Greifensee, an upper limit for the photodegradation kinetics could be found ($k_{field} \leq$ 0.01 $day^{-1}$; Tixier et al., 2003). By comparison, one has $k_{APEX}$ = 0.06±0.02 $day^{-1}$ (AQ2S) and $k_{APEX}$ = 0.018±0.006 $day^{-1}$ (CBBP). In all the cases, a better agreement with the field/experimental data could be obtained by using the CBBP compared to the AQ2S proxy.

## Conclusions

Compared to AQ2S, the use of CBBP as a proxy of $^3$CDOM* reactivity allows for more meaningful estimates to be obtained, for the $^3$CDOM* reaction rate constants with IBP, APAP and CLO. The AQ2S-based estimates actually give rate constant values for the mentioned compounds ($k_{S,^3AQ2S^*}$, where S is a generic contaminant) that are quite above the $5\times10^9$ L mol$^{-1}$ s$^{-1}$ upper limit generally accepted for $k_{S,^3CDOM^*}$. In contrast, the corresponding values of $k_{S,^3CBBP^*}$ are coherent with the reported upper limit. Moreover, a better agreement between the modelled and the available field or experimental data of IBP and CLO photodegradation could be obtained in the CBBP compared to the AQ2S scenario. In the case of ATZ, both AQ2S and CBBP allow for similar $k_{ATZ,^3CDOM^*}$ estimates to be obtained, and the results can be compared for validation with an independent (and compatible) literature value. In addition to the rate constants of triplet sensitisation, the environmental photo-fate modelling also requires the possible back-reduction processes to be taken into account. In this work, evidence of the occurrence of back reduction was obtained only in the case of CLO.

Despite the overestimation of the $^3$CDOM* processes induced by the use of AQ2S as proxy, the qualitative conclusion that $^3$CDOM* is the main high-DOC phototransformation pathway for all the studied compounds is not much modified by replacing AQ2S with CBBP. However, the predicted photochemical lifetimes of IBP, APAP and CLO for DOC = 10 mg$_C$ L$^{-1}$ are increased by 2-5 times when using the CBBP proxy. In contrast, rather similar lifetime results are obtained for ATZ when using either the AQ2S or the CBBP proxy, because $k_{ATZ,^3CBBP^*}$ is not far from $k_{ATZ,^3AQ2S^*}$.

In conclusion, differently from the high-DOC role of $^3$CDOM*, the photochemical lifetimes of APAP, IBP and CLO at high DOC need to be reconsidered in the light of the lower estimated reactivity towards triplet-sensitised degradation.

## Acknowledgements

The stay of SC in Clermont-Ferrand was financially supported by the Erasmus Traineeship programme. The PhD scholarship of LC was financially supported by Compagnia di San Paolo (Torino, Italy).

## References

Allen, J. M., Allen, S. K., Baertschi, S. W., 2000. 2-Nitrobenzaldehyde: a convenient UV-A and UV-B chemical actinometer for drug photostability testing. J. Pharmaceut. Biomed. Anal. 24, 167-178.

Avetta, P., Fabbri, D., Minella, M., Brigante, M., Maurino, V., Minero, C., Pazzi, M., Vione, D., 2016. Assessing the phototransformation of diclofenac, clofibric acid and naproxen in surface waters: model predictions and comparison with field data. Water Res. 105, 383-394.

Bahnmueller, S., von Gunten, U., Canonica, S., 2014. Sunlight-induced transformation of sulfadiazine and sulfamethoxazole in surface waters and wastewater effluents. Water Res. 57, 183-192.

Bedini, A., De Laurentiis, E., Sur, B., Maurino, V., Minero, C., Brigante, M., Mailhot, G., Vione, D., 2012. Phototransformation of anthraquinone-2-sulphonate in aqueous solution. Photochem. Photobiol. Sci. 11, 1445-1453.

Bianco, A., Fabbri, D., Minella, M., Brigante, M., Mailhot, G., Maurino, V., Minero, C., Vione, D., 2015. New insights into the environmental photochemistry of 5-chloro-2-(2,4-dichlorophenoxy)phenol (triclosan): Reconsidering the importance of indirect photoreactions. Water Res. 72, 271-280.

Bodrato, M., Vione, D., 2014. APEX (Aqueous Photochemistry of Environmentally occurring Xenobiotics): A free software tool to predict the kinetics of photochemical processes in surface waters. Environ. Sci.: Processes Impacts 16, 732-740.

Bonnemoy, F., Lavédrine, B., Boulkamh, A., 2004. Influence of UV irradiation on the toxicity of phenylurea herbicides using microtox test. Chemosphere 54, 1183–1187.

Braslavsky, S.E., 2007. Glossary of terms used in photochemistry. third edition. Pure Appl. Chem. 79, 293-465.

Burns, J. M., Cooper, W. J., Ferry, J. L., King, D. W., DiMento, B. P., McNeill, K., Miller, C. J., Miller, W. L., Peake, B. M., Rusak, S. A., Rose, A. L., Waite, T. D., 2012. Methods for reactive oxygen species (ROS) detection in aqueous environments. Aquat. Sci. 74, 683-734.

Calza, P., Noé, G., Fabbri, D., Santoro, V., Minero, C., Vione, D., Medana, C., 2017. Photoinduced transformation of pyridinium-based ionic liquids, and implications for their photochemical behavior in surface waters. Water Res. 122, 194-206.

Canonica, S., Hellrung, B., Wirz, J., 2000. Oxidation of phenols by triplet aromatic ketones in aqueous solution. J. Phys. Chem. A 104, 1226-1232.

Canonica, S., Laubscher, H.-U., 2008. Inhibitory effect of dissolved organic matter on triplet-induced oxidation of aquatic contaminants. Photochem. Photobiol. Sci. 7, 547-551.

Carena, L., Minella, M., Barsotti, F., Brigante, M., Milan, M., Ferrero, A., Berto, S., Minero, C., Vione, D., 2017. Phototransformation of the herbicide propanil in paddy field water. Environ. Sci. Technol. 51, 2695-2704.

Cermola, M.., DellaGreca, M.., Iesce, M. R., Previtera, L., Rubino, M., Temussi, F., Brigante, M., 2005. Phototransformation of fibrate drugs in aqueous media. Environ. Chem. Lett. 3, 43-47.

Challis, J. K., Hanson, M. L., Friesen, K. J., Wong, C. S., 2014. A critical assessment of the photodegradation of pharmaceuticals in aquatic environments: defining our current understanding and identifying knowledge gaps. Environ. Sci.: Processes Impacts 16, 672-696.

De Laurentiis, E., Prasse, C., Ternes, T.A., Minella, M., Maurino, V., Minero, C., Sarakha, M., Brigante, M., Vione, D., 2014. Assessing the photochemical transformation pathways of acetaminophen relevant to surface waters: transformation kinetics, intermediates, and modelling. Water Res. 53, 235-248.

Erickson, P. R., Moor, K. J., Werner, J. J., Latch, D. E., Arnold, W. A., McNeill, K., 2018. Singlet oxygen phosphorescence as a probe for triplet-state dissolved organic matter reactivity. Environ. Sci. Technol. 52, 9170-9178.

Galichet, F., Mailhot, G., Bonnemoy, F., Bohatier, J., Bolte, M., 2002. Iron(III) photoinduced degradation of isoproturon: correlation between degradation and toxicity. Pest Manage. Sci. 58, 707–712.

Iesce, M. R., Lavorgna, M., Russo, C., Piscitelli, C., Passananti, M., Temussi, F., DellaGreca, M., Cermola, F., Isidori, M., 2019. Ecotoxic effects of loratadine and its metabolic and light-induced derivatives. Ecotoxicol. Environ. Safety 170, 664-672.

Jacobs, L. E., Fimmen, R. L., Chin, Y.-P., Mash, H. E., Weavers, L. K., 2011. Fulvic acid mediated photolysis of ibuprofen in water. Water Res. 45, 4449-4458.

Janssen, E. M. L., Erickson, P. R., McNeill, K., 2014. Dual roles of dissolved organic matter as sensitizer and quencher in the photooxidation of tryptophan. Environ. Sci. Technol. 48, 4916-4924.

Kliegman, S., Eustis, S. N., Arnold, A. W., McNeill, K., 2013. Experimental and theoretical insights into the involvement of radicals in triclosan phototransformation. Environ. Sci. Technol. 47, 6756-6763.

Koehler, B., Barsotti, F., Minella, M., Landelius, T., Minero, C., Tranvik, L. J., Vione, D., 2018. Simulation of photoreactive transients and of photochemical transformation of organic pollutants in sunlit boreal lakes across 14 degrees of latitude: a photochemical mapping of Sweden. Water Res. 129, 94-104.

Kovacic, A., Gys, C., Kosjek, T., Covaci, A., Heath, E., 2019. Photochemical degradation of BPF, BPS and BPZ in aqueous solution: Identification of transformation products and degradation kinetics. Sci. Total Environ. 664, 595-604.

Leresche, F., von Gunten, U., Canonica, S., 2016. Probing the photosensitizing and inhibitory effects of dissolved organic matter by using N,N-dimethyl-4-cyanoaniline (DMABN). Environ. Sci. Technol. 50, 10997-11007.

Loiselle, S. A., Azza, N., Cozar, A., Bracchini, L., Tognazzi, A., Dattilo, A., Rossi, C., 2008. Variability in factors causing light attenuation in Lake Victoria. Freshwater Biol. 53, 535-545.

Marchetti, G., Minella, M., Maurino, V., Minero, C., Vione, D., 2013. Photochemical transformation of atrazine and formation of photointermediates under conditions relevant to sunlit surface waters: laboratory measures and modelling. Water Res. 47, 6211-6222.

McNeill, K., Canonica, S., 2016. Triplet state dissolved organic matter in aquatic photochemistry: Reaction mechanisms, substrate scope, and photophysical properties. Environ. Sci.: Processes Impacts 18, 1381-1399.

Minella, M., Rapa, L., Carena, L., Pazzi, M., Maurino, V., Minero, C., Brigante, M., Vione, D., 2018. An experimental methodology to measure the reaction rate constants of processes sensitised by the triplet state of 4-carboxybenzophenone as a proxy of the triplet states of chromophoric dissolved organic matter, under steady-state irradiation conditions. Environ. Sci.: Processes Impacts 20, 1007-1019.

Packer, J. L., Werner, J. J., Latch, D. E., McNeill, K., Arnold, W. A., 2003. Photochemical fate of pharmaceuticals in the environment: naproxen, diclofenac, clofibric acid, and ibuprofen. Aquat. Sci. 65 (4), 342-351.

Remucal, C. K., 2014. The role of indirect photochemical degradation in the environmental fate of pesticides: A review. Environ. Sci.: Processes Impacts 16, 628-653.

Rosario-Ortiz, F. L., Canonica, S., 2016. Probe compounds to assess the photochemical activity of dissolved organic matter. Environ. Sci. Technol. 50, 12532-12547.

Schmitt, M., Erickson, P. R., McNeill, K., 2017. Triplet-state dissolved organic matter quantum yields and lifetimes from direct observation of aromatic amine oxidation. Environ. Sci. Technol. 51, 13151-13160.

Tartarotti, B., Trattner, F., Remias, D., Saul, N., Steinberg, C. E. W., Sommaruga, R., 2017. Distribution and UV protection strategies of zooplankton in clear and glacier-fed alpine lakes. Sci. Reports 7, article #4487.

Tixier, C., Singer, H .P., Oellers, S., Müller, S. R., 2003. Occurrence and fate of carbamazepine, clofibric acid, diclofenac, ibuprofen, ketoprofen, and naproxen in surface waters. Environ. Sci. Technol. 37, 1061-1068.

Verpoorter, C., Kutser, T., Seekell, D. A., Tranvik, L. J., 2014. A global inventory of lakes based on high-resolution satellite imagery. Geophys. Res. Lett. 41, 6396-6402.

Vione, D., Maddigapu, P. R., De Laurentiis, E., Minella, M., Pazzi, M., Maurino, V., Minero, C., Kouras, S., Richard, C., 2011. Modelling the photochemical fate of ibuprofen in surface waters. Water Research 45, 6725-6736.

Vione, D., 2014. A test of the potentialities of the APEX software (Aqueous Photochemistry of Environmentally-occurring Xenobiotics). Modelling the photochemical persistence of the herbicide cycloxydim in surface waters, based on literature kinetics data. Chemosphere 99, 272-275.

Vione, D., Minella, M., Maurino, V., Minero, C., 2014. Indirect photochemistry in sunlit surface waters: Photoinduced production of reactive transient species. Chemistry Eur. J. 20, 10590-10606.

Vione, D., Fabbri, D., Minella, M., Canonica, S., 2018. Effects of the antioxidant moieties of dissolved organic matter on triplet-sensitized phototransformation processes: Implications for the photochemical modeling of sulfadiazine. Water Res. 128, 38-48.

Vione, D., Koehler, B., 2018. Modelled phototransformation kinetics of the antibiotic sulfadiazine in organic matter-rich lakes. Sci. Total Environ. 645, 1465-1473.

Wang, X. H., Lin, A. Y. C., 2012. Phototransformation of cephalosporin antibiotics in an aqueous environment results in higher toxicity. Environ. Sci. Technol. 46, 12417-12426.

Wenk, J., von Gunten, U., Canonica, S., 2011. Effect of dissolved organic matter on the transformation of contaminants induced by excited triplet states and the hydroxyl radical. Environ. Sci. Technol. 45, 1334-1340.

Wenk, J., Canonica, S., 2012. Phenolic antioxidants inhibit the triplet-induced transformation of anilines and sulfonamide antibiotics in aqueous solution. Environ. Sci. Technol. 46, 5455-5462.

Wetzel, R. G., 2001. Limnology: Lake and River Ecosystems. Academic Press: Third Edition.

Weyhenmeyer, G. A., Müller, R. A., Norman, M., Tranvik, L. J., 2016. Sensitivity of freshwaters to browning in response to future climate change. Clim. Change 134, 225-239.

Williamson, C. E., Overholt, E. P., Pilla, R. M., Leach, T. H., Brentrup, J. A., Knoll, L. B., Mette, E. M., Moeller, R. E., 2015. Ecological consequences of long-term browning in lakes. Sci. Rep. 5, article n. 18666.

Yan, S., Song, W., 2014. Photo-transformation of pharmaceutically active compounds in the aqueous environment: A review. Environ. Sci.: Processes Impacts 16, 697-720.

Yassine, M., Fuster, L., Devier, M. H., Geneste, E., Pardon, P., Grelard, A., Dufourc, E., Al Iskandarani, M., Ait-Aissa, S., Garric, J., Budzinski, H., Mazellier, P., Trivella, A. S., 2018. Photodegradation of novel oral anticoagulants under sunlight irradiation in aqueous matrices. Chemosphere 193, 329-336.

Zeng, T., Arnold, A., 2013. Pesticide photolysis in prairie potholes: probing photosensitized processes. Environ. Sci. Technol. 47, 6735-6745.